Pharmacogn. Mag.
A multifaceted peer reviewed journal in the field of Pharmacognosy and Natural Products
www.phcog.com | www.phcog.net

ORIGINAL ARTICLE

Herniarin, a Natural Coumarin, Inhibits Mammary Carcinogenesis by Modulating Liver X Receptor-α/β-PI3K-Akt-Maf1 Pathway in Sprague-Dawley Rats

Pritha Bose, Shakti Prasad Pattanayak

Division of Advanced Pharmacology, Department of Pharmaceutical Sciences and Technology, BIT Mesra, Ranchi, Jharkhand, India

Submitted: 26-06-2019 Revised: 26-08-2019 Published: 28-11-2019

ABSTRACT

Background: The massive tumor burden following breast cancer initiation requires a constant supply of energy achieved by modification of different metabolic pathways. Enhanced lipid synthesis associated with glucose metabolism modification triggered by a battery of signaling events promotes unregulated cell division and growth. Coumarins with their diversified bioactivity are also recognized for their therapeutic efficacy in breast cancer. **Objectives:** Thus, this study was performed to assess the chemotherapeutic potential of herniarin (HER), a 7-methoxycoumarin derivative against polycyclic aromatic hydrocarbon-induced mammary cancer. **Materials and Methods:** *In silico* molecular docking was carried out to identify the interactions of HER with LXR α and β, 3-hydroxy-3-methylglutaryl-coenzyme A reductase (HMGCoAR), PI3K, and Akt followed by *in vitro* evaluation of HMGCoAR inhibitory potential of HER. Detailed *in vivo* studies was then performed in 7,12-dimethylbenz(a) anthracene-induced breast cancer model in Sprague-Dawley (SD) rats using HER at doses 20 mg/kg, b. w. and 40 mg/kg, b. w. along with molecular-level analysis (messenger RNA and proteins) by real-time quantitative polymerase chain reaction, Western blot, and enzyme-linked immunosorbent assay. **Results:** The docking studies revealed a significant binding affinity of HER to the aforesaid receptors and its HMGCoAR inhibitory potential (IC_{50} = 103.1 nM) validated the docking studies. HER successfully re-established the lipid and lipoprotein levels along with the activities of lipid-metabolizing enzymes and glycolytic enzymes that were altered following cancer induction. The molecular biology evaluations reflected the efficiency of HER as it evidently alleviated the overexpression of HMGCOAR, PI3K, and Akt along with the lipogenic genes fatty acid synthase and acetyl-CoA carboxylase 1 in the carcinoma-developed animals by upregulating LXR (α and β) and Maf1. **Conclusion:** The bioactive moiety HER efficiently controlled alterations in metabolic pathways, thus balancing energy consumption, attenuating tumor progression through LXR/PI3K/Akt/Maf1 axis in breast cancer in SD rats.

Key words: 7,12-dimethylbenz(a)anthracene, herniarin, lipid and glucose metabolism, lipid and glucose metabolism (α and β), mammary cancer

SUMMARY

- Agonistic action of HER to liver X receptor (α and β) is associated with inhibition of PI3K/Akt pathway. Triggering of LXR mediates Maf1 upregulation which in turn is involved in suppression of fatty acid synthase and acetyl-CoA carboxylase 1 (lipogenic genes), thus preventing lipid biogenesis. LXR activation also causes impediment of PI3K-Akt pathway, thus restricting glucose uptake. Maf1 upregulation inhibits tumorigenesis. HER also accounts for inhibition of 3-hydroxy-3-methylglutaryl-coenzyme A reductase. Thus, HER binds to LXR and inhibits breast cancer through PI3K/Akt/Maf1 axis.

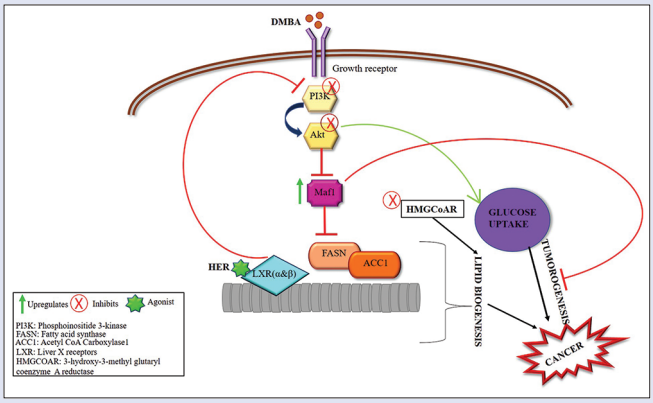

Abbreviations used: HER: Herniarin; LXR: Liver X receptor; HMGCoAR: 3-hydroxy-3-methylglutaryl-coenzyme A reductase; FASN: Fatty acid synthase; ACC1: Acetyl-CoA carboxylase 1; RT-qPCR: Real-time quantitative polymerase chain reaction.

Correspondence:

Dr. Shakti Prasad Pattanayak,
Department of Pharmaceutical Sciences and Technology, Division of Advanced Pharmacology, BIT Mesra, Ranchi - 835 215, Jharkhand, India.
E-mail: sppattanayak@bitmesra.ac.in
DOI: 10.4103/pm.pm_264_19

Access this article online
Website: www.phcog.com
Quick Response Code:

INTRODUCTION

Breast cancer is globally proclaimed as the most frequently occurring invasive malignancy among women in the 21st century.[1] It is the second most prevalent malignancy following lung cancer, and breast cancer alone is anticipated to be responsible for 29% of all newly diagnosed cancers in women.[2] According to the recent advances in Medical Science, breast cancer is defined as a heterogeneous and multifarious disease with diversified histological as well as mutational characteristics which are distinctly classified in molecular subtypes of clinical significance. Animals with chemically induced cancer, specifically

Cite this article as: Bose P, Pattanayak SP. Herniarin, a natural coumarin, inhibits mammary carcinogenesis by modulating liver X receptor-α/β-PI3K-Akt-Maf1 Pathway in sprague-dawley rats. Phcog Mag 2019;15:S510-9.

rodents, are widely used as a reliable animal model for evaluating diagnostic and/or chemotherapeutic efficacy of different candidate drugs. Marked resemblance with the histopathological characteristics and steps involved in progression of tumor in human carcinogenesis confers the rodent models to be extensively explored in the field of cancer studies.[3] Polycyclic aromatic hydrocarbons (PAHs) which majorly constitute the environmental carcinogens are found responsible for mammary carcinoma. A prototype of PAH, 7,12-dimethylbenz(a) anthracene (DMBA), is reported for successful promotion of breast cancer in animal models[4,5] which is generally administered to young rodents with undifferentiated mammary glands when cellular proliferation rates are high that increase the chances for breast cancer development.[6] The intermediates produced by DMBA metabolism are responsible for forming stable mutagenic DNA adducts involved in cancer initialization.[7] Cancer cells are typically characterized by elevated glucose uptake along with reactivated *de novo* biosynthesis of lipids. This alteration in metabolic phenotype acts as a hallmark for cancer cells, thus distinguishing them from the nonproliferative healthy tissues of the body. In addition to the multiple structural functions coordinated by lipids, they are also a key factor in various cell signaling pathways as well as cell-to-cell communication. On the other hand, glucose, one of the fundamental modulators of energy generation is also involved in contributing essential biosynthetic precursors, for example, ribosomes prerequisite for nucleotide production essential for DNA and RNA synthesis. Thus, comprehension of the metabolic outcomes of lipids and glucose in facilitating survival and growth of cancer cells may unfold new therapeutic avenues for cancer treatment.[8] Macromolecules such as lipids, proteins, and nucleic acid synthesis typically identify the abnormal growth and proliferation of cells. Cells must undergo metabolic alterations allowing synthesis of active intermediates that serve as a precursor assisting biomass production.[8] Different oncoproteins and associated signaling pathways target various lipogenic and glycolytic enzyme expressions that result in enhanced glucose utilization as well as production of fatty acid derivatives leading to metabolic reprogramming in initial stage of various cancers.[9]

Previous studies have revealed an intimate association of abnormalities in lipid levels to that of cancer development and metastasis. Altered metabolism of lipids induced to fulfill the soaring energy demands required for accelerated cellular proliferation or malignant transformation leads to cancer cell survival.[10] *De novo* lipid synthesis is also a consistent source of this energy demand.[11] Proliferating cancer cells needs large amount of cholesterol that results in increased consumption and biogenesis of lipids causing accelerated biosynthesis of cholesterol. Activation of liver X receptors (LXR α and β) belonging to the family of nuclear receptors by oxysterols is responsible for modulating lipid synthesis along with homeostasis of cholesterol.[12] LXRs are considered as the regulatory hub monitoring diverse pathways accompanying metabolism of energy, cholesterol, and also fatty acids.[13,14] Thus, LXRs being activated are accountable for maintaining and normalizing cellular cholesterol status through molecular signaling pathways that are either involved in controlling uptake or reverse transportation of cholesterol.[15]

On the other hand, high glucose consumption (aerobic glycolysis) is another atypical characteristic of cancer cells.[16] Metabolites arising from elevated glucose consumption and glycolytic activity, normally responsible for adenosine triphosphate (ATP) generation, are redirected to biosynthetic including lipid pathways. This high rate of metabolism accelerates the proliferation in cancer cells which is termed as Warburg effect.[17] The LXRs are also associated in conservation of glucose homeostasis by synchronizing signaling pathways involved in metabolism of glucose and thus may act as a potential therapeutic target for coordinating both lipid and glucose metabolism in carcinogenesis.

With recent advances in phytochemical research, a wide variety of bioactive moieties have been identified with antioxidant, chemopreventive anti-inflammatory anticancer and other therapeutic properties. The advantages exhibited by these bioactive moieties that mainly include lower toxicity along with minimalization of conventional dose of drug have attracted the attention of researchers which may help in succeeding the impediments intertwined with the current chemotherapeutics. Thus, in the present study, we have focused on coumarin family of phytochemicals that are reported to have *in vitro* inhibitory activity in malignant tumor cell lines and also shows promising *in vivo* antiproliferative potential against various mammalian tumors.[18,19] Clinical trials also revealed their therapeutic efficacy in various types of cancer including breast cancer.[20] Herniarin (HER), a 7-methoxycoumarin derivative, is reported of having diversified pharmacological properties including anti-inflammatory,[21] radical scavenging,[22] antinociceptive,[23] and cytotoxic activities[24-29] in various cell lines including MCF-7 and laryngeal cancer cell lines. However, till date, to our best knowledge, HER has not been explored for detailed *in vivo* evaluation to enlighten the mechanistic pathways contributing to its chemotherapeutic potential. The current study deals with *in silico* molecular docking analysis of HER followed by detailed *in vitro, in vivo* (in DMBA-promoted mammary carcinoma model in Sprague-Dawley [SD] rats) along with molecular biology studies for evaluation of its activity in LXR/PI3K/Akt/Maf1. Axis thus identifies its chemotherapeutic potential in attenuating breast cancer.

MATERIALS AND METHODS

Materials

DMBA (D3254-100 mg) and HER were purchased from Sigma-Aldrich (W515809) (St. Louis, MO, USA). Every reagent utilized in this study was assured of being highly pure and of analytical grade.

In silico molecular docking analysis of herniarin on liver X receptor-α, liver X receptor-β, 3-hydroxy-3-methylglutaryl-coenzyme A reductase, P13K, and Akt

All docking calculations of HER were performed in AutoDock 4.0. The protein coordinates of LXR-α (PDB ID: 5AVL), LXR-β (PDB ID: 18PD), 3-hydroxy-3-methylglutaryl-coenzyme A reductase (HMGCoAR) (PDB ID: 1HW9), PI3K (PDB ID: 5ESH), and Akt (PDB ID: 5KCV) were retrieved from PDB repository. Geometries were preprocessed for correcting the bond orders and protonation states and adding missing atoms in standard amino acids, using Maestro module of Schrodinger suite. Gasteiger-Marsili charges were used for docking calculation. Grid spacing of 0.37 Å was used, centering the reference ligands of each protein system for grid preparation using AutoGrid. Lamarckian genetic algorithm (LGA) along with LUDI-type scoring function was employed as a search engine – 100 LGA runs to obtaining the docking pose.

In vitro evaluation of 3-hydroxy-3-methylglutaryl-coenzyme A reductase inhibitory potential of herniarin

The HMGCoAR inhibitory potential of HER was evaluated using HMGCoAR assay kit (Sigma-Aldrich) as per manufacturer's guidance. The reference control used was Pravastatin. Briefly, NADPH (4 µL) and HMGCoAR substrate (12 µL) were made up to 0.2 ml (final volume) using potassium phosphate buffer (100 mM, pH 7.4) (consisting of 120 mM KCl, 1 mM Ethylene diamine tetra-acetic acid [EDTA], and 5 mM dithiothreitol [DTT]) and were started (time 0) following the addition of human recombinant HMGCoAR (2 µL) (catalytic domain which

is provided in the kit). Following this, the reaction was subsequently incubated in the presence/absence of HER (dissolved in dimethyl sulfoxide) at 37°C. The rate of NADPH consumption was observed for 15 min (at a time span of 20 s each). Calculation of IC_{50} value and % inhibitory enzymatic activity was done by the following equation:

%Inhibition = (A [control] − A [test])/A [control]) ×100, where A = Absorbance.

Experimental animals

In the current study, 50–55-day-old female (virgin) SD rats were procured from the Central Animal Facility, Birla Institute of Technology (BIT) Mesra, Ranchi, Jharkhand, India (Reg. No. 1968/PO/Re/S/17/CPCSEA and IAEC Protocol Approval No. 1972/PH/BIT/20/17/IAEC). The study was conducted with prior approval from the Institutional Animal Ethics Committee, BIT Mesra, Ranchi, India. The standard laboratory quality and conditions were maintained for the experimental animals throughout the entire study period with unlimited access to water and food.

In vivo study design

Random distribution of animals was performed such that six SD rats were included in each of four experimental groups. Control rats in Group I were administered with only vehicle (olive oil [0.5 ml] on the day of induction and treatment involved 1% sodium carboxymethyl cellulose [CDH, New Delhi, India]). Cancer was induced in SD rats belonging to Group II (induced control) through slightly modified air pouch technique[30] and received 20 mg DMBA (suspended in 0.5 mL olive oil). Animals belonging to Groups III and IV were categorized as treatment groups and received HER (20 and 40 mg/kg, b. w, i. p., respectively) The treatment was continued for 28 days following promotional stage (90 days) from administration of DMBA with regular weekly monitoring of body weight as well as tumor location by palpation following induction process. After completion of treatment protocol, collection of blood samples from all the experimental rats was done by retro-orbital puncture followed by isolating serum and plasma for further biochemical analysis. Then, the animals were sacrificed and perfused with subsequent isolation of liver and mammary tissues. Sections of tissue were homogenized using neutral phosphate-buffered saline having pH 7 while other fractions of breast tissue were cautiously preserved in liquid nitrogen for future enzyme-linked immunosorbent assay (ELISA), real-time quantitative polymerase chain reaction (RT-qPCR), and Western blotting.

Biochemical quantification of lipids, lipoproteins, and lipid-metabolizing enzymes

The technique of Folch *et al.*[31] was followed for extracting lipids, and the plasma Folch aliquots were used to determine the lipid components. The method of Van Handle[32] was modified a little to estimate triglyceride (TG). Rouser *et al.*[33] method was employed for evaluating phospholipids (PLs). For estimation of total cholesterol (TC), Parekh and Jung method[34] was followed while free cholesterol (FC) was analyzed according to enzymic scheme proposed by Leffler and McDougald. Free fatty acid (FFA) estimation was performed as per the principle of Horn and Menahan.[35] Dual precipitation technique mediated the fractionization of plasma lipoproteins. Adding heparin-magnesium to plasma precipitated very-low-density lipoprotein-cholesterol (VLDL-C) and low-density lipoprotein-cholesterol (LDL-C), while the high-density lipoprotein-cholesterol (HDL-C) in supernatant was quantified in fraction. Quantification of lipoprotein lipase (LL) in plasma and tissue samples was carried out according to Huttunen *et al.* technique[36] along with estimation of total lipase in both plasma and tissue samples. The procedure postulated by Kothari *et al.*[37] was implemented to evaluate cholesterol ester synthase (CES) and cholesterol ester hydrolase (CEH). And finally, for analyzing lecithin–cholesterol acyltransferase (LCAT) activity, Latha *et al.*[38] method was implemented.

Assessment of glycolytic enzymes in different experimental groups of animals

The hexokinase (HK) activity in terms of nmol of glucose-6-phosphate liberated per mg protein was determined at 340 nm. Aldolase (AL) activity was determined according to Sibley and Lehninger protocol.[39] Hydrazine (dinitrophenyl hydrazine) traps the formed triosephosphates to produce colored dinitrophenyl hydrazone which was estimated at 540 nm.

3-hydroxy-3-methylglutaryl-coenzyme A reductase enzyme determination by enzyme-linked immunosorbent assay

Assessment of HMGCoAR of the animals was performed with corresponding ELISA kit as claimed by the manufacturer (Cell Applications, Inc., San Diego, CA, USA).

Investigation of messenger RNA expressions of 3-hydroxy-3-methylglutaryl-coenzyme A reductase enzyme, liver X receptor-α, liver X receptor-β, PI3K, Akt, Maf1, fatty acid synthase, and acetyl-CoA carboxylase through real-time quantitative polymerase chain reaction

The sections of breast tissues, being thoroughly washed with phosphate-buffered saline, were subjected for total RNA extraction using TRIzol reagent (Sigma-Aldrich, Bangalore, India) and was preserved for 2 h at −80°C.[40] This was followed by 15 min centrifuging at 13,000 rpm for isolating purified RNA at 4°C. Synthesis of complementary DNA was successively followed using (Bio-Rad RT-PCR kit) total RNA (1 μg) as per instructions. The qPCR of all genes was carried out with the help of dTTP utilizing the 2x SYBR qPCR Master Mix (Kapa Biosystems) with specific forward and backward primers, as mentioned in Table 1. The cycling conditions maintained for HMGCoAR, LXR-α, LXR-β, Maf1, PI3K, Akt, fatty acid synthase (FASN), and acetyl-CoA carboxylase 1 (ACC1) were given as follows: one cycle at 95°C for 3 min, 39 cycles of 95°C for 10 s, and 58°C for 30 s. The appearance of a single peak in the melting curve analyses (60.0–95.0°C, increment 0.5°C, for 0.05) validated specificity of PCR amplification. Each RT-qPCR experiment was conducted three times. Glyceraldehyde-3-phosphate dehydrogenase was considered as an internal control.

Western blot analysis for liver X receptor-α, liver X receptor-β, Maf1, PI3K, and p-Akt in breast tissues

Following washing thrice the sections of breast tissue preserved in liquid nitrogen using phosphate-buffered saline, 10 min of lysis was performed using ice-cold lysis buffer (500 μL) comprising 50 mM NaCl, 0.5 M sucrose, 10 mM HEPES (pH 7.9), 0.1 mM EDTA, 0.5% triton, 1 mM DTT, 1 mM phenylmethylsulfonyl fluoride (PMSF), 5 μL protease inhibitor, and 5 μL of phosphatase inhibitor cocktails. This was followed by 10 min centrifuging (1000 rpm) cell lysates at 4°C with subsequent protein quantification by employing Bradford protein assay.[40] Proceeding this, sodium dodecyl sulfate–polyacrylamide gel electrophoresis was conducted using equivalent proportions of protein samples followed by transferring electrophoretically the separated proteins to nitrocellulose membrane (Millipore). 5% w/v non-fat dry

Table 1: Forward and backward primer sequences of messenger RNA for real-time quantitative polymerase chain reaction analysis

	mRNA	Primer	Sequence (5′ > 3′)	Location
1	HMGCoAR	Forward primer	CTGGAATTATGAGTGCCCCAAA	135-156
		Reverse primer	ACGACTGTACTGAAGACAAAGC	329-308
2	LXR-α	Forward primer	CTCAATGCCTGATGTTTCTCCT	21-42
		Reverse primer	TCCAACCCTATCCCTAAAGCAA	170-149
3	LXR-β	Forward primer	ATGTCTTCCCCCACAAGTTCT	1-21
		Reverse primer	GACCACGATGTAGGCAGAGC	156-137
4	Maf1	Forward primer	AGCTACTCGTGTAAGATGGCG	91-111
		Reverse primer	CTGCACTTGTCGCTCAGAG	266-248
5	PI3K	Forward primer	AAAGGCCGAGCCCTCTATTAT	10-30
		Reverse primer	GGACAATCTCGACGTAAGAAGC	178-157
6	Akt	Forward primer	TGGGTTCAGAAGAGGGGAGAA	31-51
		Reverse primer	AGGGGATAAGGTAAGTCCACATC	152-130
7	FASN	Forward primer	GGAGGTGGTGATAGCCGGTAT	6-26
		Reverse primer	TGGGTAATCCATAGAGCCCAG	145-125
8	ACC1	Forward primer	CTTCCTGACAAACGAGTCTGG	4587-4607
		Reverse primer	CTGCCGAAACATCTCTGGGA	4818-4799
9	GAPDH	Forward primer	TGGATTTGGACGCATTGGTC	333-352
		Reverse primer	TTTGCACTGGTACGTGTTGAT	543-523

mRNA: Messenger RNA; LXR: Liver X receptor; HMGCoAR: 3-hydroxy-3-methylglutaryl-coenzyme A reductase; FASN: Fatty acid synthase; ACC1: acetyl-CoA carboxylase 1; GAPDH: Glyceraldehyde 3-phosphate dehydrogenase; Maf1: proto-oncogene c-Maf or V-Maf musculoaponeurotic fibrosarcoma oncogene homolog; PI3K: Phosphoinositide 3-kinase; Akt: a serine/threonine-protein kinase

milk in Tris-buffered saline Tween-20 (TBST; 5% w/v) was then used for blocking the non-specific sites of the blots for 1 h at room temperature. Then, the primary antibodies were used for overnight incubation of the blots at 4°C. This was followed by washing thrice the blots thoroughly each for 5 min with TBST prior to their 1 h re-incubation with 1:20,000 dilution of Horse Radish Peroxide (HRP)-conjugated secondary antibody at room temperature. Then membranes development was carried out with chemiluminescent substrate (Thermo Fisher Scientific) followed by acquiring on film (CL-XPosure, 8 × 10in). The following primary antibodies at predetermined dilution were used against LXR-α, LXR-β, PI3K, p-Akt, Maf1, and β-actin (Cell Signaling Technology, Danvers, MA, USA) 1:500 in 5% w/v Bovine serum albumin (BSA) in TBST. Densitometry analysis was performed with Image J software (NIH, Washington, USA). β-actin was kept as internal control.

Statistical analysis

Analysis of all the obtained data was done by one-way analysis of variance followed by Bonferroni's multiple comparison tests with a similar sample size ($n = 6$). The variation was regarded significant when $P < 0.05$. All the values were expressed as mean ± standard error of mean.

RESULTS

Molecular docking and binding pattern analysis

Following software validation by redocking, docking simulations of HER was performed with the LXR-α, LXR-β, HMGCoAR, PI3K, and Akt active sites [Supplementary Figure 1a-c]. The *in silico* studies illustrated the interaction of HER with LXR-α [Figure 1a] forming hydrogen bond with Phe257 and hydrophobic interactions with Met298, Ile295, Leu299, Ala261, Ile339, and Leu299; with LXR-β [Figure 1b] forming hydrogen bond with Glu281 and hydrophobic interactions with Phe243, Phe333, Leu330, and Leu274; and with HMGCoAR [Figure 1c] forming hydrogen bond with Glu559 and hydrophobic interactions with Leu562, Lys561, and Ala 856. Docking analysis of reference molecule and HER with PI3K (Supplementary Figure 1d; Figure 1d respectively) and with Akt (Supplementary Figure 1e; Figure 1e respectively) showed that the active sites of PI3K and AKT was occupied by HER in a similar a fashion as that of the reference molecule. Thus, these above-mentioned interactions indicate HER to have significant binding affinity to corresponding receptors, thus validating its efficacy [Supplementary Table 1].

Herniarin inhibited 3-hydroxy-3-methylglutaryl -coenzyme A reductase activity *in vitro*

HER with IC_{50} value of 103.1 ($n = 3$) was successful in inhibiting HMGCoAR activity, while the Pravastatin which was used as a positive control revealed an IC_{50} value of 72.71($n = 3$) [Figure 2a].

Herniarin restored back 7,12-dimethylbenz(a) anthracene-induced body weight (b. w.) changes and inhibited mammary tumorigenesis of breast cancer-bearing animals

The weekly changes in body weight recorded for the entire study protocol are illustrated in [Figure 2b]. Gradual and normal increase in b. w. was evident in Group I animals. Though in the initial 6–7 weeks of proliferation stage, the b. w. of cancer-induced animals in Group II was found to increase gradually, the latter stage was marked with subsequent reduction in b. w that was highly significant ($P < 0.001$) with reference to the Group I animals at the end of 118 days. However, HER treatment successfully normalized the altered body weight in a dose-dependent fashion with animals in Group IV receiving HER (40 mg/kg b. w., i. p.) demonstrating maximum protection. Assessments of tumorigenesis in all experimental animals are shown in Figure 2c. Following cancer induction, animals in Group II developed large-sized tumor which was significantly reduced ($P < 0.001$) with increasing dose of HER as revealed by Group IV animals.

Herniarin reversed the abnormalities in lipid levels of experimental animals

The outcome following cancer induction and concurrent HER treatment on lipid profile was evaluated from the alterations in TG, PL, TC, FC, FFA, and EC levels, as demonstrated in Figure 3a. Plasma samples indicated notably ($P < 0.001$) elevated respective lipid levels in Group II (induced control) animals with respect to that of Group I rats. With the increasing dose of HER, animals in treatment Groups III and IV, respectively, revealed attenuation of the concerned lipid profile. While HER (20 mg/kg b. w., i. p.) significantly ($P < 0.01$) reduced lipid levels in comparison to the induced control group, HER (40 mg/kg b. w., i. p) enumerated maximum protection, thus almost normalizing back the lipids status with insignificant ($P > 0.05$) difference in reference to Group I animals.

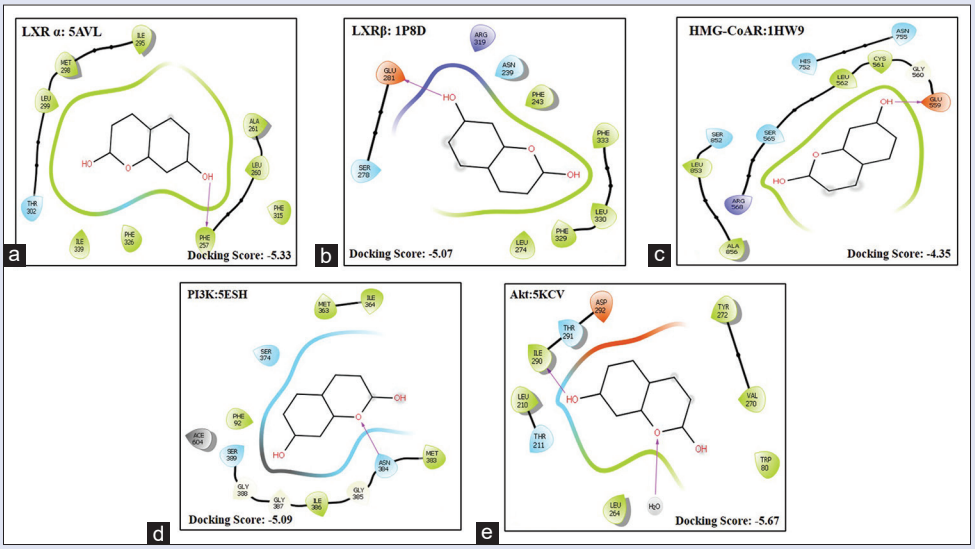

Figure 1: Molecular docking analysis of HER where (a) two-dimensional interactive diagram of HER at the active site of LXR-α (PDB ID: 5AVL), (b) two-dimensional interactive diagram of HER at the active site of LXR-β (PDB ID: IP8D), (c) two-dimensional interactive diagram of HER at the active site of HMGCoAR (PDB ID: 1HW9), (d) two-dimensional interactive diagram of HER at the active site of PI3K (PDB ID: 5ESH), (e) two-dimensional interactive diagram of HER at the active site of Akt (PDB ID: 5KCV). HER: Herniarin; LXR: Liver X receptor; HMGCoAR: 3-hydroxy-3-methylglutaryl-coenzyme A reductase; PI3K: Phosphoinositide 3-kinase

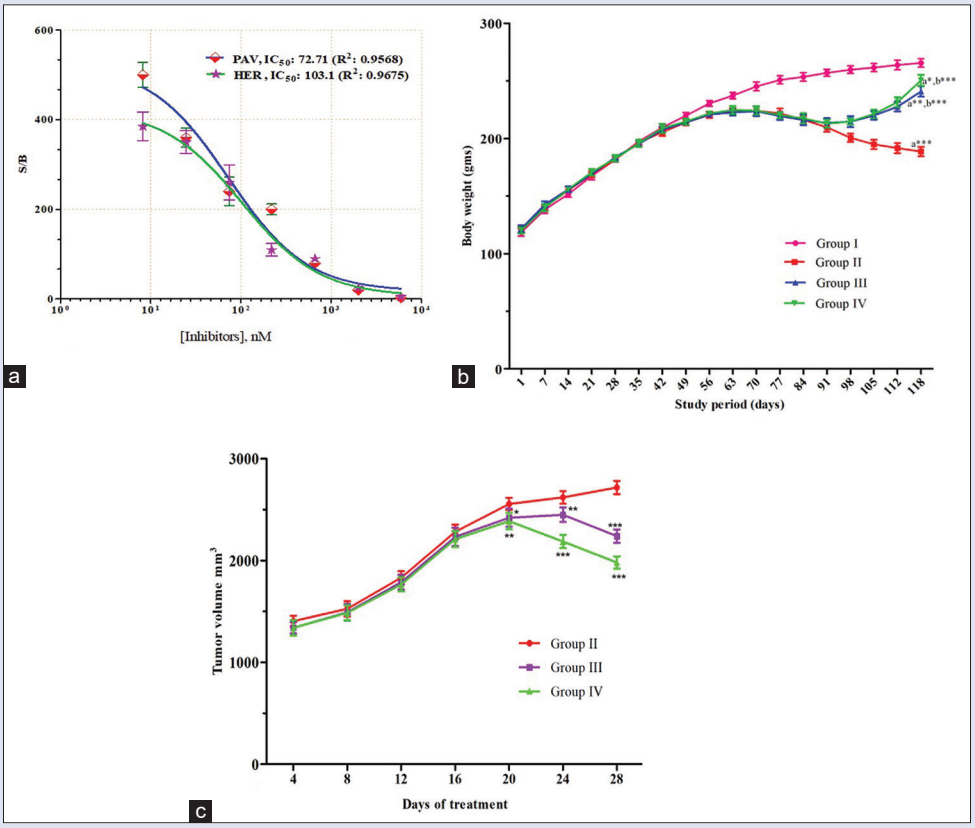

Figure 2: (a) *In vitro* 3-hydroxy-3-methylglutaryl-coenzyme A reductase (inhibitory activity of herniarin ($IC_{50:}$ 103.1 nM) (n = 3), (b) Effect of herniarin on body weight (g) of cancer-induced rats where each value shows mean ± standard error of mean (n = 6); comparisons: a – Groups II, III, and IV compared with Group I; b – Groups III and IV compared to Group II, (c) effect of herniarin on tumor weight of cancer bearing rats where each value shows mean ± standard error of mean (n = 6); comparisons: groups III and V compared with Group II; ***P < 0.001; **P < 0.01; *P < 0.05; ^{ns}P > 0.05; Group I – Control; Group II – Induced control (DMBA, 20 mg); Group III – DMBA (20 mg) + herniarin (20 mg/kg, b. w.); Group IV – DMBA (20 mg) + herniarin (40 mg/kg b. w.). DMBA: 7,12-dimethylbenz(a)anthracene

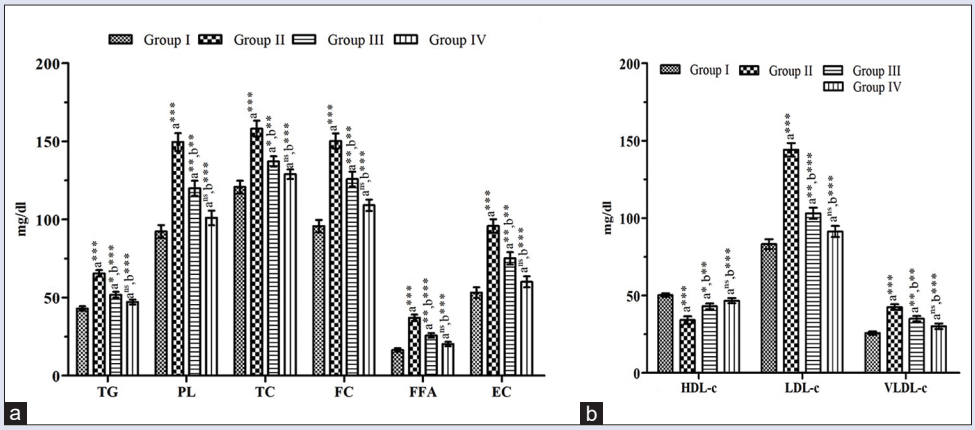

Figure 3: Effect of herniarin treatment on lipids and lipoprotein levels. Where (a) estimation of plasma lipids (TG, PL, TC, FC, FFA, and EC) and (b) Estimation of plasma lipoproteins (HDL-C, LDL-C, and VLDL-C) in all experimental groups of animals where each value shows mean ± standard error of mean ($n = 6$); comparisons: a – Groups II, III, and IV compared with Group I; b – Groups III and IV compared to Group II; ***$P < 0.001$; **$P < 0.01$; *$P < 0.05$; $^{ns}P > 0.05$; Group I – Control; Group II – Induced control (DMBA, 20 mg); Group III – DMBA (20 mg) + herniarin (20 mg/kg, b. w.); Group IV – DMBA (20 mg) + herniarin (40 mg/kg b. w.). DMBA: 7,12-dimethylbenz(a)anthracene; TG: Triglyceride; PL: Phospholipid; TC: Total cholesterol; FC: Free cholesterol; FFA: Free fatty acid; EC: Ester cholesterol; HDL-C: High-density lipoprotein-cholesterol; LDL-C: Low-density lipoprotein-cholesterol; VLDL-C: Very-low-density lipoprotein-cholesterol

Herniarin reverted lipoprotein levels in experimental groups of animals

Plasma lipoprotein analysis following DMBA induction and HER treatment in experimental groups of SD rats is represented in Figure 3b. Animals in Group II exhibited significantly ($P < 0.001$) declined level of HDL-C with marked ($P < 0.001$) concurrent rise in LDL-C and VLDL-C in contrast to the animals of Group I. On comparing with Group II, HER treatment caused dose-dependent reversion of the altered lipoprotein levels in Groups III and IV, respectively, with the highest dose of HER efficiently restoring back the lipoprotein levels toward normalcy ($P > 0.05$) when compared to Group I animals.

Herniarin treatment modulated the lipid-metabolizing enzymes in breast cancer-bearing rats

Lipid-metabolizing enzymes (LMEs) being signature enzymes for comprehending lipid biotransformation, the outcome of carcinogen administration, and HER treatment on LME activity (both plasma and liver tissues) were evaluated, and the results are represented in Figure 4a and b, respectively. Both plasma and liver samples of the induced control (Group II) animals revealed the LCAT and LL activity to be remarkably decreased ($P < 0.001$) with subsequently elevated ($P < 0.001$) TL activity in contrast to the control (Group I) rats. Moreover, the liver samples also demonstrated CEH and CES being highly ($P < 0.001$) raised in Group II SD rats following cancer induction. However, the animals administered with HER in Groups III and IV exhibited the concerned enzyme activities to be reserved back almost toward normalcy as the highest dose of HER proved to show maximum protection resulting in nonsignificant difference ($P > 0.05$) with that of control (Group I) animals.

Herniarin ameliorated the changes glycolytic enzymes profile of 7,12-dimethylbenz(a) anthracene-induced animals

Excess utilization of glucose being the identifying feature of cancer cells makes quantification of HK and AL an essential parameter in the different groups of animals under study. The results are given in Figure 4c. Following cancer induction Group II animals demonstrated significantly augmented ($P < 0.001$) HK and AL levels in comparison with control group animals. HER treatment (20 mg/kg b. w., i. p.) in Group III caused significant reduction of the glycolytic levels ($P < 0.01$) in comparison to Group II while 40 mg/kg b. w., i. p. HER administration in Group IV resulted in highly significant alleviation of HK and AL levels, thereby almost normalizing the glycolytic status as that of control animals.

Herniarin restored alterations in messenger RNA expressions of liver X receptor-α, liver X receptor-β, Maf1, 3-hydroxy-3-methylglutaryl-coenzyme A reductase, PI3K, p-Akt, fatty acid synthase, and acetyl-CoA carboxylase 1 in cancer-bearing animals

The *in silico* molecular docking results has been supported and confirmed on *in vivo* grounds by elucidating the influence of HER treatment on LXR-α, LXR-β, Maf1, HMGCoAR, PI3K, p-Akt, FASN, and ACC1 messenger RNA (mRNA) expressions in breast tissues of the animals being studied. The results are represented in Supplementary Figure 2. While LXR-α, LXR-β, and Maf1 mRNA expressions were evidently ($P < 0.001$) downregulated in Group II animals, there was also significant overexpression ($P < 0.001$) of HMGCoAR, PI3K, Akt, FASN, and ACC1 mRNA with respect to control rats. Increasing doses of HER in Groups III and IV, respectively, led to efficient restoration of all the mRNA expressions in dose-dependent fashion when compared to Group II animals. Thus, HER exhibited promising efficacy in almost normalizing the altered mRNA expressions with insignificant variation between the control groups.

Effect of herniarin on protein expressions of liver X receptor-α, liver X receptor-β, Maf1, PI3K, p-Akt, and 3-hydroxy-3-methylglutaryl-coenzyme A reductase in cancer-developed animals

The influence of HER treatment on protein expression of LXR-α, LXR-β, Maf1, PI3K, and p-Akt has been determined by Western blot while HMGCoAR expression was evaluated by ELISA. Comparing with the control group, highly significant (P<0.001) downregulation of LXR alpha [Figure 5a], LXR beta [Figure 5b], and Maf1 [Figure 5c] protein expression was observed in animals bearing breast cancer with

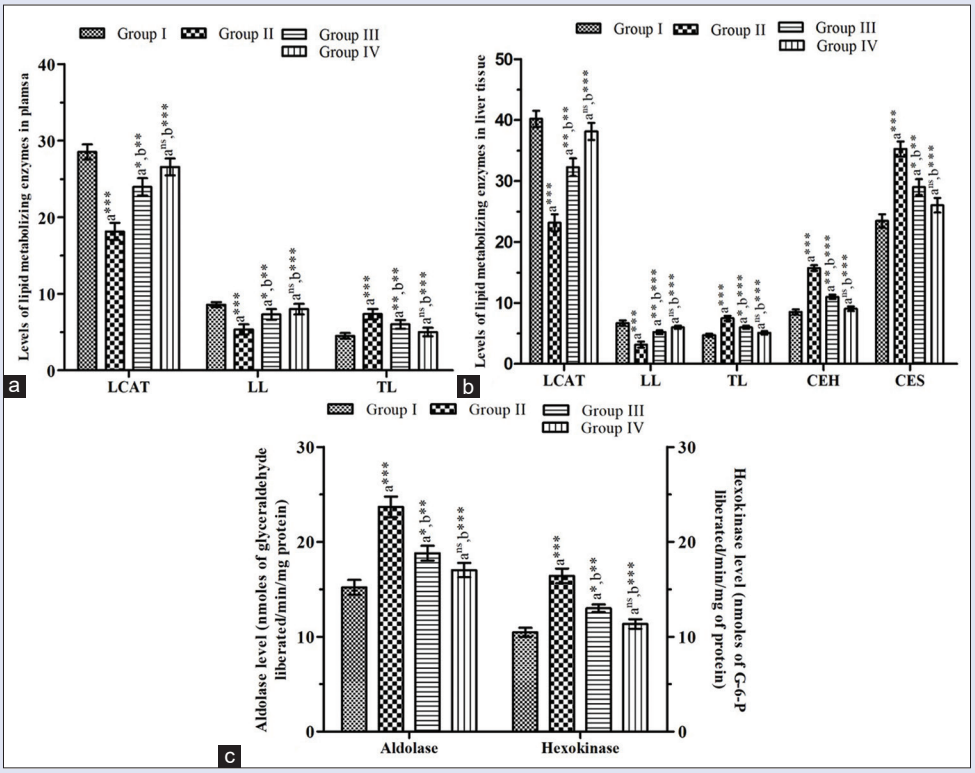

Figure 4: Herniarin restored the altered lipid-metabolizing enzyme and glycolytic enzymes. Where (a) analysis of LCAT, LL, and TL activity in plasma samples, (b) analysis of LCAT, LL, TL, CES, and CEH activity in liver tissue samples, and (c) estimation of HK and AL of all groups of animals where each value shows mean ± standard error of mean ($n = 6$); where a – Groups II, III, and IV compared with Group I; b – Groups III and IV compared to Group II; ***$P < 0.001$; **$P < 0.01$; *$P < 0.05$; $^{ns}p > 0.05$; Group I – Control; Group II – Induced control (DMBA, 20 mg), Group III – DMBA (20 mg) + herniarin (20 mg/kg, b. w.); Group IV – DMBA (20 mg) + herniarin (40 mg/kg, b. w.). DMBA: 7,12-dimethylbenz(a)anthracene; LCAT: lecithin–cholesterol acyltransferase; LL: Lipoprotein lipase; TL: Total lipase; CES: Cholesterol ester synthetase; CEH: Cholesterol ester hydrolase; HK: Hexokinase; AL: Aldolase

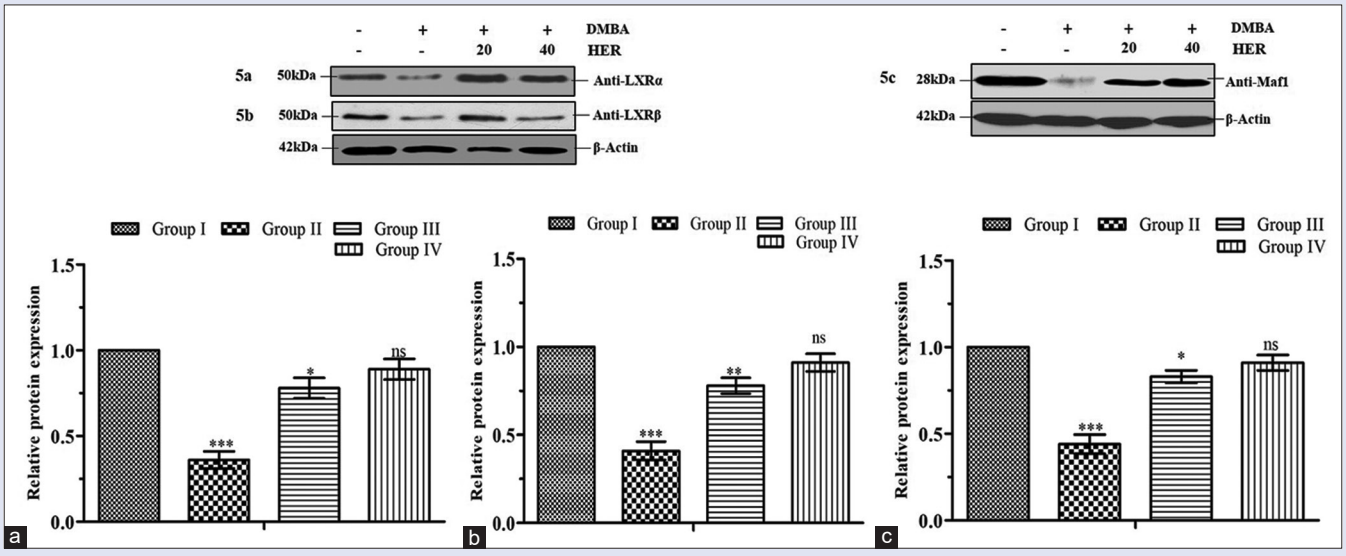

Figure 5: Effect of herniarin on protein expressions of LXR-α, LXR-β, and Maf1 in mammary tissues of experimental animals. Where (a) relative protein expression for LXR-α, (b) relative protein expression for LXR-β, (c) relative protein expression for Maf1 where each value shows mean ± standard error of mean ($n = 6$); where a – Groups II, III, and IV compared with Group I; b – Groups III and IV compared to Group II; ***$P < 0.001$; **$P < 0.01$; *$P < 0.05$; $^{ns}p > 0.05$; Group I – Control; Group II – Induced control (DMBA, 20 mg), Group III – DMBA (20 mg) + herniarin (20 mg/kg, b. w.); Group IV – DMBA (20 mg) + herniarin (40 mg/kg, b. w.). DMBA: 7,12-dimethylbenz(a)anthracene, LXR: Liver X receptor

expressions of PI3K [Figure 6c], p-AKT [Figure 6B] and HMGCoAR being subsequently upregulated. Following treatment with HER, the animals in Group III and IV demonstrated significant ($P < 0.001$) and dose-dependent amelioration of these abnormalities in protein

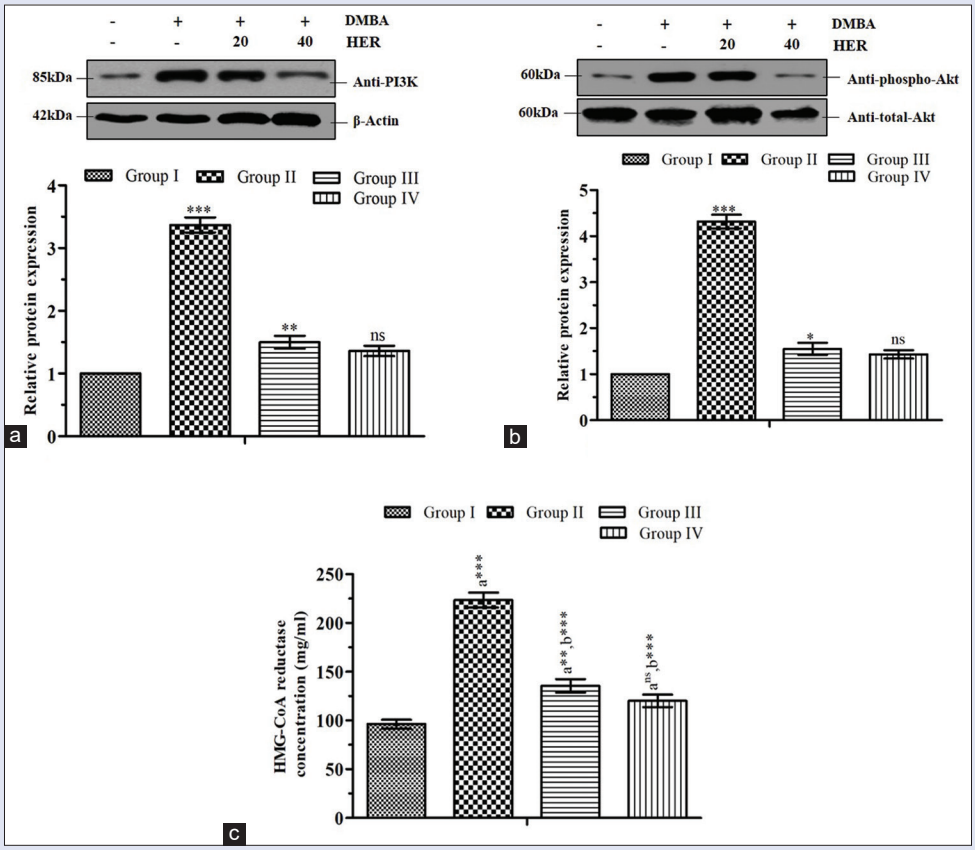

Figure 6: Effect of herniarin on protein expressions of PI3K, Akt, and HMGCoAR in mammary tissues of all experimental animals. Where (a) relative protein expression for PI3K, (b) relative protein expression for Akt. Where each value shows mean ± standard error of mean (n = 6); where Groups II, III, and IV compared with Group I. (c) relative protein expression for HMGCoAR where each value shows mean ± standard error of mean (n = 6); where, a – Groups II, III, and IV compared with Group I; b – Groups III and IV compared to Group II; ***P < 0.001; **P < 0.01; *P < 0.05; ^{ns}P > 0.05; Group I – Control; Group II – Induced control (DMBA, 20 mg), Group III – DMBA (20 mg) + herniarin (20 mg/kg, b. w.); Group IV – DMBA (20 mg) + herniarin (40 mg/kg, b. w.). DMBA: 7,12-dimethylbenz(a)anthracene; PI3K: phosphoinositide 3-kinase; HMGCoAR: 3-hydroxy-3-methylglutaryl-coenzyme A reductase

expression in Group II, thereby establishing HER as a potent chemotherapeutic biomoiety.

DISCUSSION

The massive tumor burden following cancer initiation requires a constant supply of energy achieved by modification of different metabolic pathways. Thus, glucose metabolism modification associated with enhanced lipid synthesis facilitating unregulated cell division along with lipid biosynthetic gene mutation serves as an identifying feature of cancer cells.[41] LXRs playing a central role in coordinating both lipid and glucose homeostasis imply the crucial role of LXR agonist in modifying the related metabolic pathways.[42] Therefore, in the current study, we evaluated the chemotherapeutic efficacy of a coumarin derivative, HER as LXR receptor agonist implementing its activity on PI3K/Akt/Maf1 axis.

Among the various oncogenic signaling pathways, PI3K/Akt/mTOR axis is annotated to have dual and critical roles in regulating both lipogenic and glycolytic pathways.[8,40,43] Phosphorylation of protein kinase Akt that assists cell survival is reduced following LXR activation in the lipid raft platform.[44] Ligand-coupled activation of LXR is also accompanied by diminished Akt activity, thus decreasing the cholesterol pool leading to apoptosis. On the other hand, Akt being a key regulator of insulin signaling is involved in glucose removal from bloodstream to different target tissues.[45] Increased glucose level necessary for cancer cells is previously reported to be expedited by cancer by Akt through various mechanisms.[8,46,47] Phosphorylation of multiple protein kinases in this PI3K-Akt pathway has been found to be attenuated by triggering of LXR, thereby inhibiting the randomly proliferating breast cancer cells.[48] Our study also revealed that HER-mediated activation of LXRs evident from their upregulated mRNA and protein expressions resulted in subsequent downregulation of mRNA and protein expressions of both PI3K and Akt. These outcomes also corroborate with the agonistic activity of HER on LXR (α and β) receptors from the docking analysis.

Maf1, a downstream signaling protein to Akt serves as a key factor linking metabolism of lipids and oncogenic transfiguration by its capability in suppressing genes involved in lipid synthesis and biosynthetic magnitude regulation. This dependency of oncogenic mutation on lipid synthesis is due to regulatory influence of PI3K/Akt signaling on expression of Maf1 involved in coordination between lipid and protein biogenesis. Maf1 upregulation in the liver of experimental mice has proved in alleviating insulin-dependent *de novo* lipogenesis.[49] Maf1 is also reported to balance intracellular accumulation of lipids. Knocking down Maf1 in mammalian cell line exhibited allied upregulation in expression of its downstream lipogenic genes, FASN and ACC1 with concomitant fatty acid accumulation.[49] Enhanced Maf1 expression in the liver of mice fed on high-carbohydrate diet attenuated increment in TGs, FASN, and ACC1. Maf1 is also involved in regulation of other multiple aspects of lipid metabolism as reported previously.[49,50] Concurrent to these

results, the present study also elucidated that cancer-induced augmented expression of oncogenic proteins PI3K, Akt, of the PI3K-Akt pathway suppressed Maf1 expression along with raised FASN and ACC1. However, HER as LXR agonist successfully reversed back these abnormalities. This molecular mechanistic efficacy of HER validates its docking results with respective proteins.

These alterations of oncogenic genes were also reflected in the *in vitro* study and different biochemical estimations performed. Cancer cells are often associated with reprogramming of cholesterol. LXRs are reported to maintain cholesterol balance within cells. Inactivation of LXR permits cholesterol agglomeration helping in synthesis of new membrane for dividing cells.[51] Cholesterol is a principal component of lipid rafts that intercede multiple signaling in cancer, and its metabolism can be targeted for developing newer therapeutic approach in breast cancer.[52] The rate limiting enzyme of cholesterol synthesis, HMGCoAR along with its specific inhibitors statins have received considerable attention in cancer research recently.[53] Increased HMGCoAR indicates enhanced isoprenoid demand for maintaining the growth of cancer cells. Thus, the inhibitory potential of LXR agonist HER against HMGCoAR analyzed in the current study showed positive results. The proliferating and migrating breast cancer cells are accelerated by lipids and lipoproteins[54] with their intensified levels being correlated in DMBA-induced breast cancer in SD rats.[35] The proteins and enzymes accountable to synthesize these lipids and lipoproteins are often activated, overexpressed or undergo alteration due to dysregulation of varied intermediate pathways. Previous researches demonstrated elevated plasma levels of TG, TC, LDL, and VLDL of breast cancer patients.[55] While accumulation of CE is responsible for promoting proliferation of mammary carcinoma cells.[56] LDL and VLDL are also recognized to facilitate breast cancer progression. On the other hand, modulation of LMEs also contributes in carcinogenesis. In patients suffering from cancer, faulty esterification of LCAT increases the FC-to-EC ratio that determines intracellular movement of cholesterol.[57] FC along with TG is cleared from blood circulation by LCAT and LL. Following breast cancer induction, animals demonstrated higher TC, TG, and FC levels which signified decline in fat-splitting enzyme expression. Moreover, the escalated total lipid contents that characterize progressive cancer caused TL activity to increase which was also clearly evident from our results. Thus, in accordance with the previous reports, the lipid, lipoproteins, and LME status that were clearly altered in breast cancer animals were significantly improved by HER.

As discussed earlier, the pathway regulating glucose metabolism also serves as a major source of energy (ATP) of cancer cells. Overexpression of HK in tumor cells increases glycolysis helping in cell proliferation.[58] The multifunctional protein HK has an integral part in regulating transcription and apoptosis. Akt-mediated mobilization of glucose transported to cellular membrane increases uptake of glucose with activated HK that phosphorylates and traps intracellular glucose. Cancer tissues are reported to express all AL isoforms with AL A being the most prominent.[59] AL knockdown has shown the most drastic consequences on proliferating cells. Thus, blocking of glycolytic enzymes may help in reversing glucose consumption promoted by cancer tissues.[40] The upsurge in HK and AL observed following cancer induction in animals was predominantly lowered by HER illustrating its chemotherapeutic potential in LXR axis.

CONCLUSION

As per the current findings, HER efficiently controlled the breast carcinogenesis in SD rats by attenuating cancer-promoted alterations in energy regulations and associated tumor progression. The detailed *in silico* docking, *in vitro*, *in vivo,* and molecular studies substantiate the efficacy of coumarin derivative HER as a potential LXR receptor agonist, thereby postulating its role as tumor static and chemotherapeutic agent that prevents proliferation by modulating P13K/Akt/Maf1 pathway.

Acknowledgements

The authors are immensely thankful to the BIT for offering all the necessary facilities and infrastructure for uninterrupted conduct of this work.

Financial support and sponsorship

This research was fully funded by AICTE under the project grant No. 8-69/RIFD/RPS/POLICY-1/2016-17.

Conflicts of interest

There are no conflicts of interest.

REFERENCES

1. Chiou YS, Li S, Ho CT, Pan MH. Prevention of breast cancer by natural phytochemicals: Focusing on molecular targets and combinational strategy. Mol Nutr Food Res 2018;62:e1800392.
2. Miller KD, Siegel RL, Lin CC, Mariotto AB, Kramer JL, Rowland JH, *et al.* Cancer treatment and survivorship statistics, 2016. CA Cancer J Clin 2016;66:271-89.
3. Balmain A, Harris CC. Carcinogenesis in mouse and human cells: Parallels and paradoxes. Carcinogenesis 2000;21:371-7.
4. Currier N, Solomon SE, Demicco EG, Chang DL, Farago M, Ying H, *et al.* Oncogenic signaling pathways activated in DMBA-induced mouse mammary tumors. Toxicol Pathol 2005;33:726-37.
5. Buters J, Quintanilla-Martinez L, Schober W, Soballa VJ, Hintermair J, Wolff T, *et al.* CYP1B1 determines susceptibility to low doses of 7,12-dimethylbenz[a] anthracene-induced ovarian cancers in mice: Correlation of CYP1B1-mediated DNA adducts with carcinogenicity. Carcinogenesis 2003;24:327-34.
6. Russo IH, Russo J. Role of hormones in mammary cancer initiation and progression. J Mammary Gland Biol Neoplasia 1998;3:49-61.
7. Anbuselvam C, Vijayavel K, Balasubramanian MP. Protective effect of *Operculina turpethum* against 7,12-dimethyl benz(a)anthracene induced oxidative stress with reference to breast cancer in experimental rats. Chem Biol Interact 2007;168:229-36.
8. Brault C, Schulze A. The role of glucose and lipid metabolism in growth and survival of cancer cells. Recent Results Cancer Res 2016;207:1-22.
9. Menendez JA, Lupu R. Fatty acid synthase and the lipogenic phenotype in cancer pathogenesis. Nat Rev Cancer 2007;7:763-77.
10. Zhu Y, Aupperlee MD, Zhao Y, Tan YS, Kirk EL, Sun X, *et al.* Pubertal and adult windows of susceptibility to a high animal fat diet in trp53-null mammary tumorigenesis. Oncotarget 2016;7:83409-23.
11. Hilvo M, Denkert C, Lehtinen L, Müller B, Brockmöller S, Seppänen-Laakso T, *et al.* Novel theranostic opportunities offered by characterization of altered membrane lipid metabolism in breast cancer progression. Cancer Res 2011;71:3236-45.
12. Lehmann JM, Kliewer SA, Moore LB, Smith-Oliver TA, Oliver BB, Su JL, *et al.* Activation of the nuclear receptor LXR by oxysterols defines a new hormone response pathway. J Biol Chem 1997;272:3137-40.
13. Pinto CL, Kalasekar SM, McCollum CW, Riu A, Jonsson P, Lopez J, *et al.* Lxr regulates lipid metabolic and visual perception pathways during zebrafish development. Mol Cell Endocrinol 2016;419:29-43.
14. Kaneko T, Kanno C, Ichikawa-Tomikawa N, Kashiwagi K, Yaginuma N, Ohkoshi C, *et al.* Liver X receptor reduces proliferation of human oral cancer cells by promoting cholesterol efflux via up-regulation of ABCA1 expression. Oncotarget 2015;6:33345-57.
15. Zelcer N, Hong C, Boyadjian R, Tontonoz P. LXR regulates cholesterol uptake through idol-dependent ubiquitination of the LDL receptor. Science 2009;325:100-4.
16. Warburg O, Posener K, Negelein EV. The metabolism of cancer cells. Biochem Z 1924;152:319-44.
17. Tekade RK, Sun X. The Warburg effect and glucose-derived cancer theranostics. Drug Discov Today 2017;22:1637-53.

18. Kapadia GJ, Rao GS, Ramachandran C, Iida A, Suzuki N, Tokuda H. Synergistic cytotoxicity of red beetroot (*Beta vulgaris* L.) extract with doxorubicin in human pancreatic, breast and prostate cancer cell lines. J Complement Integr Med 2013;10. pii:/j/jcim. 2013.10.issue-1/jcim-2013-0007/jcim-2013-0007.xml.
19. Kim TH, Shin YJ, Won AJ, Lee BM, Choi WS, Jung JH, *et al.* Resveratrol enhances chemosensitivity of doxorubicin in multidrug-resistant human breast cancer cells via increased cellular influx of doxorubicin. Biochim Biophys Acta 2014;1840:615-25.
20. Venkata Sairam K, Gurupadayya BM, Chandan RS, Nagesha DK, Vishwanathan B. A review on chemical profile of coumarins and their therapeutic role in the treatment of cancer. Curr Drug Deliv 2016;13:186-201.
21. Silván AM, Abad MJ, Bermejo P, Sollhuber M, Villar A. Antiinflammatory activity of coumarins from *Santolina oblongifolia*. J Nat Prod 1996;59:1183-5.
22. Bertin R, Chen Z, Martínez-Vázquez M, García-Argaéz A, Froldi G. Vasodilation and radical-scavenging activity of imperatorin and selected coumarinic and flavonoid compounds from genus *Casimiroa*. Phytomedicine 2014;21:586-94.
23. Cheriyan BV Sr., Kadhirvelu P Sr., Nadipelly J Jr., Shanmugasundaram J, Sayeli V Sr., Subramanian V Sr. Anti-nociceptive effect of 7-methoxy coumarin from *Eupatorium triplinerve vahl* (Asteraceae). Pharmacogn Mag 2017;13:81-4.
24. Haghighitalab A, Matin MM, Bahrami AR, Iranshahi M, Haghighi F, Porsa H. Enhancement of cisplatin cytotoxicity in combination with herniarin *in vitro*. Drug Chem Toxicol 2014;37:156-62.
25. Valiahdi SM, Iranshahi M, Sahebkar A. Cytotoxic activities of phytochemicals from *Ferula* species. Daru 2013;21:39.
26. Jassbi AR, Firuzi O, Miri R, Salhei S, Zare S, Zare M, *et al.* Cytotoxic activity and chemical constituents of *Anthemis mirheydari*. Pharm Biol 2016;54:2044-9.
27. Hong L, Ying SH. Ethanol extract and isolated constituents from *Artemisia dracunculus* inhibit esophageal squamous cell carcinoma and induce apoptotic cell death. Drug Res (Stuttg) 2015;65:101-6.
28. Mousavi SH, Davari AS, Iranshahi M, Sabouri-Rad S, Tayarani Najaran Z. Comparative analysis of the cytotoxic effect of 7-prenyloxycoumarin compounds and herniarin on MCF-7 cell line. Avicenna J Phytomed 2015;5:520-30.
29. Kielbus M, Skalicka-Wozniak K, Grabarska A, Jeleniewicz W, Dmoszynska-Graniczka M, Marston A, *et al.* 7-substituted coumarins inhibit proliferation and migration of laryngeal cancer cells *in vitro*. Anticancer Res 2013;33:4347-56.
30. Arun B, Udayachander M, Meenakshi A. 7,12-dimethylbenzanthracene induced mammary tumours in wistar rats by 'air pouch' technique – A new approach. Cancer Lett 1984;25:187-94.
31. Folch J, Lees M, Sloane Stanley GH. A simple method for the isolation and purification of total lipides from animal tissues. J Biol Chem 1957;226:497-509.
32. Kumar A, Sunita P, Pattanayak SP. Silibinin inhibits the hepatocellular carcinoma in NDEA-induced rodent carcinogenesis model: An evaluation through biochemical and bio-structuralparameters. J Cancer Sci Ther 2015;7:1948-5956.
33. Rouser G, Fkeischer S, Yamamoto A. Two dimensional then layer chromatographic separation of polar lipids and determination of phospholipids by phosphorus analysis of spots. Lipids 1970;5:494-6.
34. Parekh AC, Jung DH. Cholesterol determination with ferric acetate-uranium acetate and sulfuric acid-ferrous sulfate reagents. Anal Chem 1970;42:1423-7.
35. Hron WT, Menahan LA. A sensitive method for the determination of free fatty acids in plasma. J Lipid Res 1981;22:377-81.
36. Huttunen JK, Ehnholm C, Kekki M, Nikkilä EA. Post-heparin plasma lipoprotein lipase and hepatic lipase in normal subjects and in patients with hypertriglyceridaemia: Correlations to sex, age and various parameters of triglyceride metabolism. Clin Sci Mol Med 1976;50:249-60.
37. Kothari HV, Bonner MJ, Miller BF. Cholesterol ester hydrolase in homogenates and lysosomal fractions of human aorta. Biochim Biophys Acta 1970;202:325-31.
38. Latha R, Shanthi P, Sachdanandam P. Kalpaamruthaa ameliorates mitochondrial and metabolic alterations in diabetes mellitus induced cardiovascular damage. J Diet Suppl 2014;11:305-19.
39. Sibley JA, Lehninger AL. Determination of aldolase in animal tissues. J Biol Chem 1949;177:859-72.
40. Haque MW, Bose P, Siddique MU, Sunita P, Lapenna A, Pattanayak SP. Taxifolin binds with LXR (α & β) to attenuate DMBA-induced mammary carcinogenesis through mTOR/Maf-1/PTEN pathway. Biomed Pharmacother 2018;105:27-36.
41. Khanna A, Pradhan A, Curran SP. Emerging roles for maf1 beyond the regulation of RNA polymerase III activity. J Mol Biol 2015;427:2577-85.
42. Laffitte BA, Chao LC, Li J, Walczak R, Hummasti S, Joseph SB, *et al.* Activation of liver X receptor improves glucose tolerance through coordinate regulation of glucose metabolism in liver and adipose tissue. Proc Natl Acad Sci U S A 2003;100:5419-24.
43. Long J, Zhang CJ, Zhu N, Du K, Yin YF, Tan X, *et al.* Lipid metabolism and carcinogenesis, cancer development. Am J Cancer Res 2018;8:778-91.
44. Zhuang L, Lin J, Lu ML, Solomon KR, Freeman MR. Cholesterol-rich lipid rafts mediate akt-regulated survival in prostate cancer cells. Cancer Res 2002;62:2227-31.
45. Manning BD, Cantley LC. AKT/PKB signaling: Navigating downstream. Cell 2007;129:1261-74.
46. Gottlob K, Majewski N, Kennedy S, Kandel E, Robey RB, Hay N. Inhibition of early apoptotic events by akt/PKB is dependent on the first committed step of glycolysis and mitochondrial hexokinase. Genes Dev 2001;15:1406-18.
47. Majewski N, Nogueira V, Bhaskar P, Coy PE, Skeen JE, Gottlob K, *et al.* Hexokinase-mitochondria interaction mediated by akt is required to inhibit apoptosis in the presence or absence of bax and bak. Mol Cell 2004;16:819-30.
48. Hassan TS, Pannicia A, Russo V, Steffensen KR. LXR inhibits proliferation of human breast cancer cells through the PI3K-Akt pathway. Nucl Receptor Res 2015;2:1-10.
49. Palian BM, Rohira AD, Johnson SA, He L, Zheng N, Dubeau L, *et al.* Maf1 is a novel target of PTEN and PI3K signaling that negatively regulates oncogenesis and lipid metabolism. PLoS Genet 2014;10:e1004789.
50. Khanna A, Johnson DL, Curran SP. Physiological roles for mafr-1 in reproduction and lipid homeostasis. Cell Rep 2014;9:2180-91.
51. Bensinger SJ, Bradley MN, Joseph SB, Zelcer N, Janssen EM, Hausner MA, *et al.* LXR signaling couples sterol metabolism to proliferation in the acquired immune response. Cell 2008;134:97-111.
52. Ding X, Zhang W, Li S, Yang H. The role of cholesterol metabolism in cancer. Am J Cancer Res 2019;9:219-27.
53. Moonindranath S, Shen H. Statins and breast cancer: An overview of the current situation. Adv Breast Cancer Res 2016;5:14.
54. Baenke F, Peck B, Miess H, Schulze A. Hooked on fat: The role of lipid synthesis in cancer metabolism and tumour development. Dis Model Mech 2013;6:1353-63.
55. Wei LJ, Zhang C, Zhang H, Wei X, Li SX, Liu JT, *et al.* A case-control study on the association between serum lipid level and the risk of breast cancer. Zhonghua Yu Fang Yi Xue Za Zhi 2016;50:1091-5.
56. de Gonzalo-Calvo D, López-Vilaró L, Nasarre L, Perez-Olabarria M, Vázquez T, Escuin D, *et al.* Intratumor cholesteryl ester accumulation is associated with human breast cancer proliferation and aggressive potential: A molecular and clinicopathological study. BMC Cancer 2015;15:460.
57. Subbaiah PV, Liu M, Witt TR. Impaired cholesterol esterification in the plasma in patients with breast cancer. Lipids 1997;32:157-62.
58. Rempel A, Mathupala SP, Griffin CA, Hawkins AL, Pedersen PL. Glucose catabolism in cancer cells: Amplification of the gene encoding type II hexokinase. Cancer Res 1996;56:2468-71.
59. Ritterson Lew C, Tolan DR. Targeting of several glycolytic enzymes using RNA interference reveals aldolase affects cancer cell proliferation through a non-glycolytic mechanism. J Biol Chem 2012;287:42554-63.